arXiv:1408.0921v3 [nucl-th] 6 Feb 2015

Azimuthal Anisotropy Distributions in High-Energy Collisions

Li Yan,[1] Jean-Yves Ollitrault,[1] and Arthur M. Poskanzer[2]

[1] *CNRS, URA2306, IPhT, Institut de physique théorique de Saclay, F-91191 Gif-sur-Yvette, France*
[2] *Lawrence Berkeley National Laboratory, Berkeley, California, 94720*

(Dated: February 9, 2015)

Elliptic flow in ultrarelativistic heavy-ion collisions results from the hydrodynamic response to the spatial anisotropy of the initial density profile. A long-standing problem in the interpretation of flow data is that uncertainties in the initial anisotropy are mingled with uncertainties in the response. We argue that the non-Gaussianity of flow fluctuations in small systems with large fluctuations can be used to disentangle the initial state from the response. We apply this method to recent measurements of anisotropic flow in Pb+Pb and p+Pb collisions at the LHC, assuming linear response to the initial anisotropy. The response coefficient is found to decrease as the system becomes smaller and is consistent with a low value of the ratio of viscosity over entropy of $\eta/s \simeq 0.19$. Deviations from linear response are studied. While they significantly change the value of the response coefficient they do not change the rate of decrease with centrality. Thus, we argue that the estimate of η/s is robust against non-linear effects.

I. INTRODUCTION

The large magnitude of elliptic flow, v_2, in relativistic heavy-ion collisions at RHIC [1] and LHC [2] has long been recognized as a signature of hydrodynamic behavior of the strongly-interacting quark-gluon plasma [3]. v_2 is understood as the hydrodynamic response to the initial anisotropy, ε_2, of the initial density profile [4]. However, the magnitude of this anisotropy is poorly constrained theoretically [5, 6]. This uncertainty hinders the extraction of the properties of the quark-gluon plasma from experimental data [7, 8].

The statistical properties of anisotropic flow are now precisely known [9]. The ATLAS collaboration has analyzed the full probability distribution of v_2, v_3 and v_4 in Pb+Pb collisions for several centrality windows [10]. In p+Pb collisions, information is less detailed, but the first moments of the distribution of v_2 have been measured [11]. Our goal is to make use of these measurements to separate the initial state from the response without assuming any particular model of the initial conditions – by only using a simple functional form which goes to zero at the geometric limits of $\varepsilon_n = 0$ and 1.

In theory, one can describe the particles emitted from a collision with an underlying probability distribution [12]. Anisotropic flow, v_n, is defined as the $n^{\rm th}$ Fourier coefficient of the azimuthal probability distribution $\mathcal{P}(\varphi)$:

$$V_n = v_n e^{in\Psi_n} \equiv \frac{1}{2\pi}\int_0^{2\pi} \mathcal{P}(\varphi) e^{in\varphi} d\varphi, \qquad (1)$$

where we have used a complex notation [13, 14]. Note that the underlying probability distribution $\mathcal{P}(\varphi)$ and V_n fluctuate event to event, but they are both theoretical quantities which cannot be measured on an event-by-event basis. The particles that are detected in an event represent a finite sample of $\mathcal{P}(\varphi)$, and the measurement of the probability distribution of v_n involves a nontrivial unfolding of statistical fluctuations [10].

II. DISTRIBUTION OF ε_n

We assume that the fluctuations of v_n for $n = 2, 3$ are due to fluctuations of the initial anisotropy ε_n in the corresponding harmonic, defined by [15]

$$\mathcal{E}_n = \varepsilon_n e^{in\Phi_n} \equiv -\frac{\int r^n e^{in\phi}\rho(r,\phi) r dr d\phi}{\int r^n \rho(r,\phi) r dr d\phi}. \qquad (2)$$

where $\rho(r,\phi)$ is the energy density near midrapidity shortly after the collision, and (r,ϕ) are polar coordinates in the transverse plane, in a coordinate system where the energy distribution is centered at the origin.

We assume for the moment that v_n in a given event is determined by linear response to the initial anisotropy, $v_n = \kappa_n \varepsilon_n$, where κ_n is a response coefficient which does not fluctuate event to event. Event-by-event hydrodynamic calculations [16] show that this is a very good approximation for $n = 2, 3$. Within this approximation, it has already been shown that one can rule out particular models of the initial density using either a combined analysis [17, 18] of elliptic flow and triangular flow [19] data, or the relative magnitude of elliptic flow fluctuations [20–22]. Our goal is to show that one can extract both κ_n and the distribution of ε_n from data. We hope to show that this is true even if we relax the linear assumption. We make use of the recent observation that the distribution of ε_n is to a large extent universal [23, 24] and can be characterized by two parameters.

Both the magnitude and direction of $\mathcal{E}_n$ fluctuate event to event. The simplest parametrization of these fluctuations is a two-dimensional Gaussian probability distribution which, upon integration over azimuthal angle, yields the Bessel-Gaussian distribution [25]:

$$p(\varepsilon_n) = \frac{\varepsilon_n}{\sigma^2} I_0\left(\frac{\varepsilon_0 \varepsilon_n}{\sigma^2}\right) \exp\left(-\frac{\varepsilon_0^2 + \varepsilon_n^2}{2\sigma^2}\right), \qquad (3)$$

where ε_0 is the mean anisotropy in the reaction plane, which vanishes by symmetry for odd n, and σ is the typical magnitude of eccentricity fluctuations around this

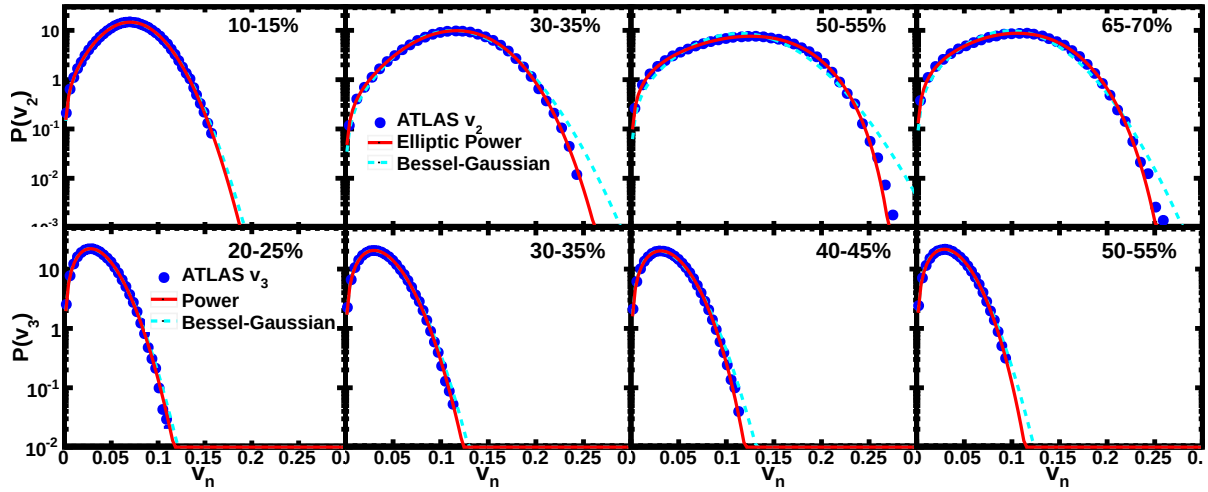

FIG. 1. (Color online) Distribution of v_2 (top) and v_3 (bottom) in various centrality windows. Symbols: ATLAS data [10] for Pb+Pb collisions at $\sqrt{s_{NN}} = 2.76$ TeV. For v_2, fits are rescaled Elliptic Power Eq. (4) (full lines) and Bessel-Gaussian distributions Eq. (3) (dashed lines). For v_3, fits are rescaled Power Eq. (6) (full lines) and Bessel-Gaussian distributions with $\varepsilon_0 = 0$ Eq. (5) (dashed lines).

mean anisotropy. Both ε_0 and σ depend on the harmonic n.

In a previous publication [24], we have introduced an alternative parametrization, the Elliptic Power distribution:

$$p(\varepsilon_n) = \frac{2\alpha\varepsilon_n}{\pi}(1-\varepsilon_0^2)^{\alpha+\frac{1}{2}} \int_0^\pi \frac{(1-\varepsilon_n^2)^{\alpha-1} d\phi}{(1-\varepsilon_0\varepsilon_n\cos\phi)^{2\alpha+1}}, \quad (4)$$

where α describes the fluctuations and is approximately proportional to the number of sources in an independent-source model [4]. The parameter α depends on n. When $\varepsilon_0 \ll 1$ and $\alpha \gg 1$, Eq. (4) reduces to Eq. (3) with $\sigma \approx 1/\sqrt{2\alpha}$. Its support is the unit disk: it naturally takes into account the condition $|\varepsilon_n| \leq 1$ which follows from the definition, Eq. (2). For this reason, it is a better parametrization than the Bessel-Gaussian, in particular for large anisotropies. Eq. (4) has been shown to fit various initial-state models [24]. Note that ε_0 is not strictly equal to the mean reaction plane eccentricity for the Elliptic Power distribution, but the difference is small for Pb+Pb collisions [24].

When the anisotropy is solely due to fluctuations, $\varepsilon_0 = 0$, the Bessel-Gaussian reduces to a Gaussian distribution:

$$p(\varepsilon_n) = \frac{\varepsilon_n}{\sigma^2}\exp\left(-\frac{\varepsilon_n^2}{2\sigma^2}\right), \quad (5)$$

and the Elliptic Power distribution reduces to the Power distribution [23]:

$$p(\varepsilon_n) = 2\alpha\varepsilon_n(1-\varepsilon_n^2)^{\alpha-1}. \quad (6)$$

III. DISTRIBUTION OF v_n

The probability distribution of anisotropic flow, $P(v_n)$, is obtained from the distribution of the initial anisotropy $p(\varepsilon_n)$ by

$$P(v_n) = \frac{d\varepsilon_n}{dv_n} p(\varepsilon_n)\,. \quad (7)$$

Assuming $v_n = \kappa_n\varepsilon_n$, this becomes:

$$P(v_n) = \frac{1}{\kappa_n} p\left(\frac{v_n}{\kappa_n}\right). \quad (8)$$

In this case the distribution is rescaled by the response coefficient κ_n. Figure 1 displays the probability distribution of v_2 and v_3 in various centrality windows [10] together with fits using rescaled Bessel-Gaussian and Elliptic Power distributions for v_2, and rescaled Gaussian and Power distributions for v_3. Both parametrizations give very good fits to v_2 and v_3 data for the most central bins shown on the figure.[1] As the centrality percentile increases, however, the quality of the Bessel-Gaussian fit becomes increasingly worse, which is reflected by the large χ^2 of the fit, and also clearly seen in the tail of the distribution: it systematically overestimates the distribution for large anisotropies. On the other hand, the Elliptic Power fit is excellent for all centralities. In particular, it falls off more steeply for large v_n, in close agreement with the data.

[1] The fits do not converge below 10% (20%) centrality for v_2 (v_3), which reflects the fact that the distributions become very close to Bessel-Gaussian (Gaussian).

Note that the Bessel-Gaussian distribution Eq. (3) is scale invariant: rescaling it by κ_n amounts to multiplying both ε_0 and σ by κ_n, so that the fit is degenerate: only the products $\kappa_n\varepsilon_0$ and $\kappa_n\sigma$ can be determined. Therefore the Bessel-Gaussian fit to ATLAS data is in practice a 2-parameter fit for v_2, and a 1-parameter fit for v_3. On the other hand, the Elliptic Power fit is not degenerate because of the non-Gaussian cut-off at $\varepsilon_n = 1$, and returns both the response coefficient κ_n and the parameters pertaining to the shape, namely α and ε_0 (for v_2). However, the fit parameters are still correlated in the sense that the combinations $\kappa_n/\sqrt{\alpha}$ and $\kappa_n\varepsilon_0$ (for v_2) have much smaller errors than each individual parameter.

IV. EXPERIMENTAL ERRORS

Our ability to separate the response from the initial eccentricity thus lies in the difference between the Bessel-Gaussian and the Elliptic Power fits, that is, in the non-Gaussianity of flow fluctuations. Since the difference is small, errors must be carefully evaluated.

The ATLAS collaboration reports the statistical error, the systematic error on the mean $\langle v_n\rangle$, and the systematic error on the relative standard deviation $\sigma_{v_n}/\langle v_n\rangle$. The first systematic error is an error on the scale of the distribution, while the second is an error on its shape. The error on the scale directly translates into an error of the response coefficient κ_n, of the same relative magnitude. Since our analysis uses the deviations from a Gaussian shape, the dominant source of error is —by far— the error on the shape. In order to estimate the corresponding error on our fit parameters, we distort the distribution of v_n in such a way that the mean $\langle v_n\rangle$ is unchanged, and $\sigma_{v_n}/\langle v_n\rangle$ is increased or decreased by the experimental uncertainty. This is done in practice by shifting the values of the v_n bins according to $v_n \to v_n + \delta(v_n)$, where $\delta(v_n)$ is a small non-linear shift. We choose the ansatz $\delta(v_n) = \epsilon v_n(v_{\rm max} - v_n)(v_n - \lambda)$, where $v_{\rm max}$ is the tail of the v_n distribution, λ is chosen in such a way that $\langle v_n\rangle$ is unchanged, and ϵ is chosen in such a way that $\sigma_{v_n}/\langle v_n\rangle$ is increased or decreased by the systematic error. This non-linear transformation leaves the minimum and maximum values of v_n invariant.

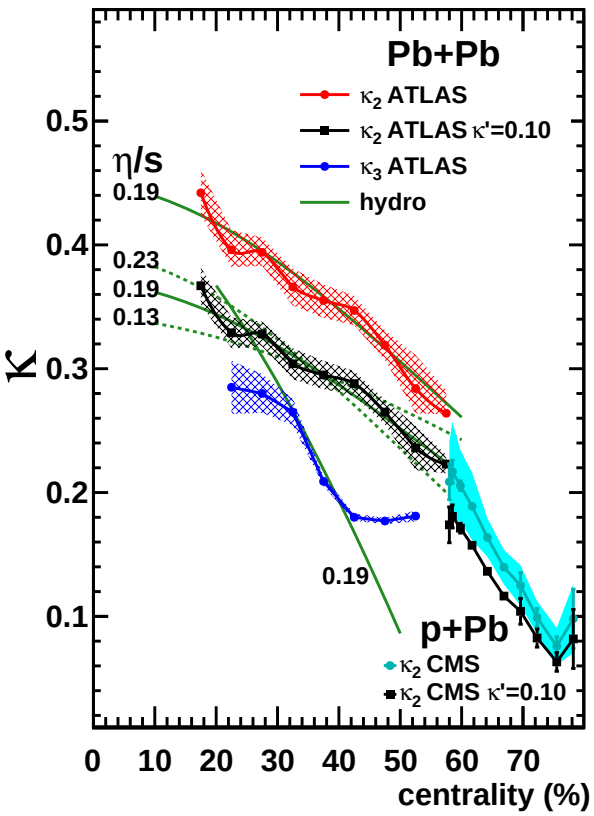

FIG. 2. (Color online) Response coefficients κ_2 and κ_3 versus centrality. Symbols: results from the fits to ATLAS Pb+Pb data [10] and to CMS p+Pb data [11]. For κ_2, systematic and statistical experimental errors are added in quadrature. For κ_3, only the statistical error is shown. Also shown are κ_2 values from fitting the v_2 distributions with a non-linear term caracterized in Eqs. (10 and 11) by κ'. The smooth solid lines are the result of a viscous hydrodynamic calculation for κ with $\eta/s = 0.19$. The upper solid line is normalized up by the factor 1.7, the middle line by the factor 1.4, and the lower line (κ_3) by the factor 3.2. The dashed lines for κ_2 with $\kappa' = 0.1$ are shown for comparison: they are for hydro results with $\eta/s = 0.13$ (normalized up by 1.2) and $\eta/s = 0.23$ (normalized up by 1.6).

V. PARAMETERS OF THE DISTRIBUTIONS

Figure 2 displays the value of the response coefficients κ_2 and κ_3 as a function of the centrality percentile. They are smaller than unity, with $\kappa_3 < \kappa_2$, in line with expectations from hydrodynamic calculations [16], and decrease as a function of the centrality percentile, which is the general behavior expected from viscous corrections to local equilibrium [26, 27]. We estimate that the low-p_T cut of ATLAS at 0.5 GeV increases κ_2 by a factor 1.4 to 1.5. The systematic error for κ_3 is very large and therefore not shown: for most bins, the upper error bar goes all the way to infinity. Now, if one takes the limit $\kappa_3 \to \infty$ while keeping the rms v_3 constant, α in Eq. (6) also goes to infinity and the Power distribution reduces to a Gaussian distribution Eq. (5). Therefore the ATLAS v_3 distributions are compatible with Gaussians within systematic errors.

The other parameters of the fit to v_n distributions, namely, ε_0 and α, characterize the shape of the distribution. They are displayed in Fig. 3 as a function of the collision centrality. ε_0 increases smoothly with the centrality percentile: extrapolation to the most central

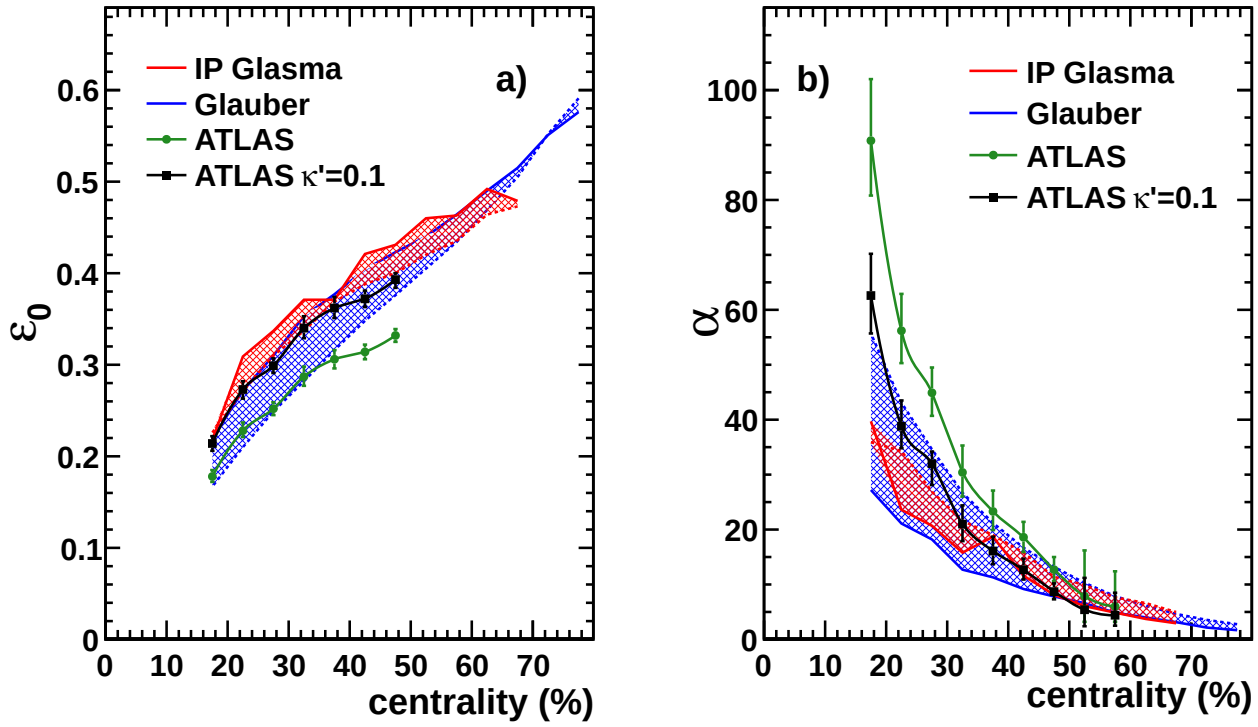

FIG. 3. (Color online) ε_0 (a) and α (b) versus centrality. Symbols: results from the fits to ATLAS v_2 data. Predictions from the Monte-Carlo Glauber [28] and IP-Glasma [29, 30] models are shown as shaded bands. Also shown are values from fits with a non-linear term defined by κ' in Eq. (10).

collisions (where the fit does not converge) gives $\varepsilon_0 = 0$, as required by azimuthal symmetry.

Figure 3 also displays comparisons with the Glauber [28, 31, 32] and IP-Glasma [29, 30] models. These models are shown as shaded bands. The bands correspond to the fact that the Elliptic Power distribution does not exactly fit the distribution of ε_2 for that particular model. Specifically, the dashed line at the edge of the band is the value returned by a 2-parameter Elliptic Power fit to the distribution of ε_2. The full line at the other edge of the band is the value that the fit to the v_2 distribution would return if $v_2 \propto \varepsilon_2$, with ε_2 given by that model. If one assumes linear response, ATLAS data deviate from both models.

VI. CUMULANTS

For p+Pb collisions, the full distribution of v_2 has not been measured, but only its first cumulants [33, 34] $v_2\{2\}$ and $v_2\{4\}$ [11, 35, 36]. Assuming linear response to the initial eccentricity, each measured cumulant is proportional to the corresponding cumulant of the initial eccentricity [37], $v_2\{k\} = \kappa_2\varepsilon_2\{k\}$, for $k = 2, 4, 6...$ The eccentricity in p+Pb collisions is solely due to fluctuations [38, 39], therefore Eqs. (5) and (6) apply. While cumulants of order 4 and higher vanish for the Gaussian distribution Eq. (5), the Power distribution Eq. (6) always gives $\varepsilon_n\{4\} > 0$ [23]. We again use this non-Gaussianity to disentangle the initial state from the response: We extract α from the measured ratio $v_n\{4\}/v_n\{2\} \simeq \varepsilon_n\{4\}/\varepsilon_n\{2\} = (1+\frac{\alpha}{2})^{-1/4}$ [23]. The rms anisotropy is then obtained as $\varepsilon_n\{2\} = 1/\sqrt{1+\alpha}$ [23]. One finally obtains for the Power distribution:

$$\kappa_n = \frac{v_n\{2\}}{\varepsilon_n\{2\}} = v_n\{2\}\sqrt{2\left(\frac{v_n\{2\}}{v_n\{4\}}\right)^4 - 1}. \qquad (9)$$

The values of κ_2 extracted from CMS p+Pb data [11] using this equation are also displayed in Fig. 2. We multiply them by a factor 1.19 to correct for the different low-p_T cut (0.3 GeV/c) assuming a linear dependence of v_2 on p_T. We plot p+Pb data at the equivalent centralities, determined according to the number of charged tracks [11]. General arguments have been put forward which suggest that the hydrodynamic response should be identical for p+Pb and Pb+Pb at the same equivalent centrality [40]. Once rescaled, the p+Pb slope is in line with Pb+Pb results, albeit somewhat steeper.

Note that the fit parameters can also be obtained

from cumulants for v_3 in Pb+Pb collisions using Eq. (9). For v_2, there is a third parameter ε_0, therefore one needs a third cumulant $v_2\{6\}$. α and ε_0, which control the shape of the distribution and its non-Gaussian features, can be extracted from the ratios $v_2\{6\}/v_2\{4\}$ and $v_2\{4\}/v_2\{2\}$ using the Elliptic Power distribution (Eq. (A5) of Ref. [24]). Note that while the Bessel-Gaussian Eq. (3) gives $\varepsilon_n\{4\} = \varepsilon_n\{6\} = \varepsilon_0$ [41], the Elliptic Power distribution always gives $\varepsilon_n\{6\} < \varepsilon_n\{4\}$. We have checked that α and ε_0 thus extracted from cumulant ratios are essentially identical to those obtained by fitting the distribution of v_2. This approach has the advantage that cumulants can be analyzed without any unfolding procedure [34] but $v_2\{2\}$ may suffer from non-flow effects.

VII. DEVIATIONS FROM LINEAR SCALING

We now discuss the effect of deviations from linear eccentricity scaling of anisotropic flow. Because of such deviations, the shape of the v_n distribution is not exactly the same as that of the ε_n distribution, as already noted in event-by-event hydrodynamic calculations [42]. There are two distinct types of non-linearities: v_n can be a function of ε_n which is not exactly linear, or v_n can depend on properties of the initial state other than ε_n. We study these effects in turn.

Adding a quadratic term would be equivalent to rotating the distribution 90 degrees or changing the sign of v_n. Thus the first significant non-linear term is the cubic:

$$v_2 = \kappa_2\varepsilon_2 + \kappa'\kappa_2\varepsilon_2^3. \tag{10}$$

Several hydrodynamic calculations show evidence that $\kappa' > 0$ [17, 43, 44], but no quantitative analysis has been done yet. One typically expects κ' to depend mildly on centrality. When fitting the experimental v_2 distributions with the added parameter of the cubic term, κ' had large errors but was in the range from 0 to 0.15. Thus we fixed κ' at 0.10 and plotted the κ_2 values also in Fig. 2. The effect of the non-linear response is to reduce the linear response coefficient κ_2, essentially by a constant factor. In the case where the distribution of ε_2 is the Power distribution (6) and in the limit $\alpha \gg 1$, the relative change of κ_2 is

$$\frac{\Delta\kappa_2}{\kappa_2} = -2\kappa' \tag{11}$$

to leading order.[2] With the Elliptic-Power distribution, the relative effect is also $\sim -2\kappa'$ as can be seen in Fig. 2. Note that this non-linear correction to the response is much larger than one would naively expect from Eq. (10): the relative magnitude of the cubic term $\kappa'\varepsilon_2^2 \ll \kappa'$, yet it produces an effect of order κ'. The reason is that the non-linear response contributes to the non-Gaussianity of flow fluctuations.

We now discuss deviations from linearity due to the fact that v_n is not entirely determined by ε_n [15]. One can generally decompose the flow as $V_n = \kappa_n\mathcal{E}_n + X_n$, where X_n is uncorrelated with the initial eccentricity $\mathcal{E}_n$. There can be various contributions to X_n from non-linear coupling between different harmonics [45] or radial modulations of the initial density [15]. In order to estimate their effect on the hydrodynamic response, we further assume that X_n is a Gaussian noise. Then, the distribution of V_n is a rescaled Elliptic-Power distribution, convoluted with a Gaussian: the deviation from linearity here results in a Gaussian smearing of the distribution.

A quantitative measure of the magnitude of X_n is the Pearson correlation coefficient r_n between the anisotropic flow and the initial anisotropy, defined as

$$\begin{aligned} r_n &\equiv \frac{\langle V_n\mathcal{E}_n^*\rangle}{\sqrt{\langle|V_n|^2\rangle\langle|\mathcal{E}_n|^2\rangle}} \\ &= \left(1 + \frac{\langle|X_n|^2\rangle}{\kappa_n^2\langle|\mathcal{E}_n|^2\rangle}\right)^{-1/2}, \end{aligned} \tag{12}$$

where angular brackets denote an average value over events in a centrality class. Our analysis assumes the maximum correlation, $|r_n| = 1$. Event-by-event hydrodynamic calculations show that there are small deviations around eccentricity scaling [46].

Ideal hydrodynamics [47] gives $|r_2| \sim 0.95$ for elliptic flow. However, the correlation between v_n and ε_n has been shown to be significantly larger in viscous hydrodynamics [16], and a value $|r_2| = 0.99$ seems reasonable, but there is to date no quantitative estimate of $|r_2|$ as defined in Eq. (12).

The effect on the fit parameters can be obtained using the fact that the rms flow $v_n\{2\} = \sqrt{\langle|V_n|^2\rangle}$ is increased by the noise, while higher-order cumulants $v_n\{4\}$ and $v_n\{6\}$ (see below Sec. VI) are unchanged. We find that a decrease of $|r_2|$ by 1% results in an decrease of the extracted κ_2 by 6% to 9%, depending on the centrality, the effect being maximum in the 20-30% centrality range. The value of $|r_2|$ found in ideal hydrodynamic calculations [47] depends mildly on centrality and is closest to 1 also in the 20-30% centrality range. Therefore one can conjecture —this should eventually be confirmed by detailed calculations— that the effect of the noise X_n is to reduce the extracted response essentially by a constant factor, independent of centrality.

Note that the cubic response in Eq. (10) does not contribute to r_2 to first order in κ', so that the two effects are in practice well separated.

The conclusion is that deviations from linear eccentricity scaling all make κ_2 smaller, by a factor which can be significant, but depends little on centrality. This is of crucial importance for the extraction of the viscosity

[2] This result is obtained by inserting Eq. (10) into Eq. (9) and using the approximate relation $\varepsilon_2\{4\}^4 \simeq \langle\varepsilon_2^6\rangle - 2\langle\varepsilon_2^4\rangle\langle\varepsilon_2^2\rangle$ for $\alpha \gg 1$.

over entropy ratio (see below). The decrease in κ_2 makes ε_0 larger and α smaller (see Fig. 3), thereby improving compatibility with existing initial-state models.

VIII. VISCOUS HYDRO

We now compare our result for κ_2 with hydrodynamic calculations. To the extent that anisotropic flow scales linearly with eccentricity, the value of the response coefficient κ_2 is independent of initial conditions. In ideal hydrodynamics, scale invariance implies that κ_2 is independent of the system size, i.e., independent of centrality. Deviations from thermal equilibrium generally result in a reduction of the flow which is stronger for peripheral collisions [26, 27]. In a hydrodynamic calculation [8], such deviations are due to the shear viscosity [7] and, to a lesser extent, to the freeze-out procedure at the end of the hydrodynamic expansion. Therefore the dependence of κ_2 on centrality in Fig. 2 can be used to estimate the shear viscosity over entropy ratio η/s of the quark-gluon plasma. We use the same hydrodynamic code as in Ref. [45] to estimate κ_2. The resulting values are significantly smaller than the data in Fig. 2. Since we have shown that deviations from linear eccentricity scaling reduce κ_2 without altering its centrality dependence, we compensate for this effect, and the low p_T cut of the ATLAS data, by multiplying our hydrodynamic result by a constant, while tuning the viscosity so as to match the centrality dependence of κ_2. Since the systematic errors on κ_3 are so large, we only fit κ_2. The smooth solid lines in Fig. 2 are obtained with $\eta/s = 0.19$. The dashed lines show the sensitivity to η/s. This extracted value of $\eta/s = 0.19$ is consistent with that reported in the literature [8], using specific models of the initial state. For sake of illustration, we also show the result for κ_3 with the same η/s and the same overall normalization factor as for κ_2. We recall that systematic errors on κ_3 from experimental data are very large so that no conclusion on η/s can be drawn from these data alone.

IX. SUMMARY

We have shown that a rescaled Elliptic Power distribution fits the measured distributions of elliptic and triangular flows in Pb+Pb collisions at the LHC. These distributions become increasingly non-Gaussian as the anisotropy increases. We have used this non-Gaussianity to disentangle for the first time the initial anisotropy from the response without assuming any particular model of initial conditions – just using a simple functional form which meets the geometrical constrants of eccentricity.

This is another aspect of the analogy between heavy-ion physics and cosmology [48, 49], where initial quantum fluctuations give rise to correlations, and the non-Gaussian statistics of these correlations can be used to unravel the properties of the initial state [50–52]. The non-Gaussianity is stronger for smaller systems, which is an incentive to analyze flow in smaller collision systems.

We have found that the hydrodynamic response to ellipticity has the expected overall magnitude and centrality dependence: it decreases with centrality percentage. A somewhat similar slope is found for p+Pb collisions. This decrease can be attributed to the viscous suppression of v_2. Comparison with hydrodynamic calculations supports a low value of the viscosity over entropy ratio, $\eta/s \sim 0.19$.

The present study can be improved by constraining the cubic response coefficient κ' in Eq. (10) as well as the Pearson coefficient due to other non-linear terms in Eq. (12). This could be done in future hydrodynamic calculations. Taking into account these nonlinear terms will decrease the magnitude of the response and therefore improve the agreement with hydrodynamic calculations. However, we have argued that this decrease is essentially a constant factor, independent of centrality, so that our estimate of η/s is likely to be robust. Our study is a first step toward the extraction of the viscosity over entropy ratio of the quark-gluon plasma from experimental data, without any prior knowledge of the initial state.

ACKNOWLEDGMENTS

We thank M. Luzum and S. Voloshin for extensive discussions and suggestions. In particular, we thank S. Voloshin for useful comments on the manuscript. JYO thanks the MIT LNS for hospitality. LY is funded by the European Research Council under the Advanced Investigator Grant ERC-AD-267258. AMP was supported by the Director, Office of Nuclear Science of the U.S. Department of Energy.

[1] K. H. Ackermann *et al.* [STAR Collaboration], Phys. Rev. Lett. **86**, 402 (2001) [nucl-ex/0009011].
[2] K. Aamodt *et al.* [ALICE Collaboration], Phys. Rev. Lett. **105**, 252302 (2010) [arXiv:1011.3914 [nucl-ex]].
[3] P. F. Kolb and U. W. Heinz, In *Hwa, R.C. (ed.) et al.: Quark gluon plasma* 634-714 [nucl-th/0305084].
[4] J. Y. Ollitrault, Phys. Rev. D **46**, 229 (1992).
[5] T. Hirano, U. W. Heinz, D. Kharzeev, R. Lacey and Y. Nara, Phys. Lett. B **636**, 299 (2006) [nucl-th/0511046].
[6] T. Lappi and R. Venugopalan, Phys. Rev. C **74**, 054905 (2006) [nucl-th/0609021].
[7] M. Luzum and P. Romatschke, Phys. Rev. C **78**, 034915 (2008) [Erratum-ibid. C **79**, 039903 (2009)] [arXiv:0804.4015 [nucl-th]].
[8] U. Heinz and R. Snellings, Ann. Rev. Nucl. Part. Sci. **63**,

123 (2013) [arXiv:1301.2826 [nucl-th]].
[9] J. Jia, arXiv:1407.6057 [nucl-ex].
[10] G. Aad *et al.* [ATLAS Collaboration], JHEP **1311**, 183 (2013) [arXiv:1305.2942 [hep-ex]].
[11] S. Chatrchyan *et al.* [CMS Collaboration], Phys. Lett. B **724**, 213 (2013) [arXiv:1305.0609 [nucl-ex]].
[12] M. Luzum and H. Petersen, J. Phys. G **41**, 063102 (2014) [arXiv:1312.5503 [nucl-th]].
[13] J. Y. Ollitrault and F. G. Gardim, Nucl. Phys. A **904-905**, 75c (2013) [arXiv:1210.8345 [nucl-th]].
[14] D. Teaney and L. Yan, Phys. Rev. C **90**, 024902 (2014) [arXiv:1312.3689 [nucl-th]].
[15] D. Teaney and L. Yan, Phys. Rev. C **83**, 064904 (2011) [arXiv:1010.1876 [nucl-th]].
[16] H. Niemi, G. S. Denicol, H. Holopainen and P. Huovinen, Phys. Rev. C **87**, 054901 (2013) [arXiv:1212.1008 [nucl-th]].
[17] B. H. Alver, C. Gombeaud, M. Luzum and J. Y. Ollitrault, Phys. Rev. C **82**, 034913 (2010) [arXiv:1007.5469 [nucl-th]].
[18] E. Retinskaya, M. Luzum and J. Y. Ollitrault, Phys. Rev. C **89**, 014902 (2014) [arXiv:1311.5339 [nucl-th]].
[19] B. Alver and G. Roland, Phys. Rev. C **81**, 054905 (2010) [Erratum-ibid. C **82**, 039903 (2010)] [arXiv:1003.0194 [nucl-th]].
[20] B. Alver *et al.* [PHOBOS Collaboration], Phys. Rev. Lett. **98**, 242302 (2007) [nucl-ex/0610037].
[21] B. Alver *et al.* [PHOBOS Collaboration], Phys. Rev. C **81**, 034915 (2010) [arXiv:1002.0534 [nucl-ex]].
[22] T. Renk and H. Niemi, Phys. Rev. C **89**, 064907 (2014) [arXiv:1401.2069 [nucl-th]].
[23] L. Yan and J. Y. Ollitrault, Phys. Rev. Lett. **112**, 082301 (2014) [arXiv:1312.6555 [nucl-th]].
[24] L. Yan, J. Y. Ollitrault and A. M. Poskanzer, Phys. Rev. C **90**, 024903 (2014) [arXiv:1405.6595 [nucl-th]].
[25] S. A. Voloshin, A. M. Poskanzer, A. Tang and G. Wang, Phys. Lett. B **659**, 537 (2008) [arXiv:0708.0800 [nucl-th]].
[26] S. A. Voloshin and A. M. Poskanzer, Phys. Lett. B **474**, 27 (2000) [nucl-th/9906075].
[27] H. J. Drescher, A. Dumitru, C. Gombeaud and J. Y. Ollitrault, Phys. Rev. C **76**, 024905 (2007) [arXiv:0704.3553 [nucl-th]].
[28] B. Alver, M. Baker, C. Loizides and P. Steinberg, arXiv:0805.4411 [nucl-ex].
[29] B. Schenke, P. Tribedy and R. Venugopalan, Phys. Rev. C **86**, 034908 (2012) [arXiv:1206.6805 [hep-ph]].
[30] B. Schenke, P. Tribedy and R. Venugopalan, Nucl. Phys. A **926**, 102 (2014) [arXiv:1312.5588 [hep-ph]].
[31] M. L. Miller, K. Reygers, S. J. Sanders and P. Steinberg, Ann. Rev. Nucl. Part. Sci. **57**, 205 (2007) [nucl-ex/0701025].
[32] W. Broniowski, P. Bozek and M. Rybczynski, Phys. Rev. C **76**, 054905 (2007) [arXiv:0706.4266 [nucl-th]].
[33] N. Borghini, P. M. Dinh and J. Y. Ollitrault, Phys. Rev. C **64**, 054901 (2001) [nucl-th/0105040].
[34] A. Bilandzic, R. Snellings and S. Voloshin, Phys. Rev. C **83**, 044913 (2011) [arXiv:1010.0233 [nucl-ex]].
[35] G. Aad *et al.* [ATLAS Collaboration], Phys. Lett. B **725**, 60 (2013) [arXiv:1303.2084 [hep-ex]].
[36] B. B. Abelev *et al.* [ALICE Collaboration], arXiv:1406.2474 [nucl-ex].
[37] M. Miller and R. Snellings, nucl-ex/0312008.
[38] P. Bozek, Phys. Rev. C **85**, 014911 (2012) [arXiv:1112.0915 [hep-ph]].
[39] P. Bozek and W. Broniowski, Phys. Lett. B **718**, 1557 (2013) [arXiv:1211.0845 [nucl-th]].
[40] G. Basar and D. Teaney, arXiv:1312.6770 [nucl-th].
[41] A. Bzdak, P. Bozek and L. McLerran, Nucl. Phys. A **927**, 15 (2014) [arXiv:1311.7325 [hep-ph]].
[42] B. Schenke and R. Venugopalan, Phys. Rev. Lett. **113**, 102301 (2014) [arXiv:1405.3605 [nucl-th]].
[43] R. S. Bhalerao, J. P. Blaizot, N. Borghini and J. Y. Ollitrault, Phys. Lett. B **627**, 49 (2005) [nucl-th/0508009].
[44] Risto Paatelainen, poster at Quark Matter 2014; Harri Niemi, plenary talk at Quark Matter 2014.
[45] D. Teaney and L. Yan, Phys. Rev. C **86**, 044908 (2012) [arXiv:1206.1905 [nucl-th]].
[46] H. Holopainen, H. Niemi and K. J. Eskola, Phys. Rev. C **83**, 034901 (2011) [arXiv:1007.0368 [hep-ph]].
[47] F. G. Gardim, F. Grassi, M. Luzum and J. Y. Ollitrault, Phys. Rev. C **85**, 024908 (2012) [arXiv:1111.6538 [nucl-th]].
[48] A. P. Mishra, R. K. Mohapatra, P. S. Saumia and A. M. Srivastava, Phys. Rev. C **77**, 064902 (2008) [arXiv:0711.1323 [hep-ph]].
[49] K. Dusling, F. Gelis and R. Venugopalan, Nucl. Phys. A **872**, 161 (2011) [arXiv:1106.3927 [nucl-th]].
[50] J. M. Maldacena, JHEP **0305**, 013 (2003) [astro-ph/0210603].
[51] N. Bartolo, E. Komatsu, S. Matarrese and A. Riotto, Phys. Rept. **402**, 103 (2004) [astro-ph/0406398].
[52] P. A. R. Ade *et al.* [Planck Collaboration], arXiv:1303.5084 [astro-ph.CO].